Eur. Polym. J. Vol. 22, No. 7, pp. 549 557, 1986
Printed in Great Britain

0014-3057/86 \$3.00 + 0.00
Pergamon Journals Ltd

CHANGES OF PROTON-ENHANCED, MAGIC-ANGLE-SPINNING ^{13}C-NMR DYNAMIC PARAMETERS DURING CURE OF TETRA(ETHYLENE GLYCOL)DIMETHACRYLATE

P. E. M. ALLEN,[1] G. P. SIMON,[1] D. R. G. WILLIAMS[2] and E. H. WILLIAMS[1,*]
[1]Department of Physical and Inorganic Chemistry and [2]Department of Chemical Engineering, University of Adelaide, Box 498 GPO, Adelaide, South Australia 5001, Australia

(*Received* 13 *November* 1985)

Abstract—Dynamic NMR and mechanical properties T_{SL}, $T_{1\rho}(C)$ at 60 kHz, T_g at ~1 Hz and its half width, log decrement (Δ_{max}) and compression modulus (E) were measured for poly[tetra(ethylene glycol)dimethacrylate] (PTEGDMA) at different extents of cure. The β, γ and water-induced transitions were also noted. The spin-lock, cross-polarization time-constant, T_{SL}, declined to its limiting value before the vitrification point. $T_{1\rho}(C)$, relaxation time in the rotating ^{13}C field, increased sharply at or just after vitrification. The change is greatest at quaternary C, decreasing through CH_2, CH_2O and CH_3, being barely significant in the latter. The observed changes affirm that $T_{1\rho}(C)$ is sufficiently influenced by spin–lattice relaxations to provide a monitor of the damping of mid kHz components during cure. The small change observed at CH_3 shows that this group is not the origin of changes in relaxation rates at other groups. Correlations with E and T_g show the importance of mid kHz components of group motion to the cooperative motions determining the response to macroscopic strain at lower frequencies. MAS ^{13}C-NMR showed that PTEGDMA contains residual unsaturation at limiting cure and that two types, constrained and unconstrained, can be distinguished.

INTRODUCTION

It is axiomatic that the origin of the bulk mechanical properties of polymers must be sought in the molecular dynamics of the macromolecules and segments of the macromolecules [1]. Proton-enhanced, magic-angle-spinning (PE/MAS) NMR techniques can provide direct information on the dynamics of particular carbon atoms in the structural unit [2, 3].

Poly[oligo(ethylene glycol)dimethacrylate] networks pass, at ambient temperatures, from brittle glasses to rubbers as the length of the flexible oligo(ethylene glycol) cross-links is increased. In the higher homologues, crystallization of the oxyethylene chains is observed [4]. They provide an excellent group for testing correlations within a homologous series. Such correlations that have been reported (e.g. [2]) have been based on a somewhat *ad hoc* selection of shop-bought polymers.

A preliminary report of results for three glycol dimethacrylates, one rubbery and two glassy, has appeared [5]. All samples appeared to be fully cured when tested by Differential Scanning Calorimetry (DSC) but PE/MAS ^{13}C-NMR spectrometry indicated that the two lower homologues contained residual unsaturation at the ultimate attainable cure. This had long been suspected [6]. PE/MAS techniques showed it to be the case and provided information about the type of unsaturation remaining.

In this paper we report the effect of extent of cure on the group dynamics of PTEGDMA. The PE/MAS time constants T_{SL} and $T_{1\rho}(C)$ have been determined in order to obtain an indication of the mobility, the "micro-Brownian motion", of each molecular group in the network.

EXPERIMENTAL

Sample preparation

Tetra(ethylene glycol)dimethacrylate (Fluka) was dried over molecular sieves for at least 1 week prior to use. De-inhibited monomer was unstable in storage even at 0°C and so inhibitor was not normally removed after we had established that the ultimate mechanical properties were unaffected when the monomer was de-inhibited by alkaline washes or passage through activated alumina. The initiator, tert-butyl per-2-ethyl hexanoate (Interox) was normally used at 0.2 vol %. Samples were cast as sheets or in curing pots, as described below, in a temperature controlled oven.

Cures were normally started at 55°C. However higher temperatures were required to attain high extents of cure, as the reaction became restricted once the T_g of the resin rose to the cure temperature.

Pot curing

In principle, the retardation of cure after vitrification could be used to devise during cycles to deliver samples of predetermined extent of cure. We used torsion-braid-analysis in order to establish the appropriate conditions. However batch reproducibility remained a problem both with inhibited and de-inhibited monomer. A collection of samples with well-spaced extents of cure were eventually obtained using specially designed curing pots, A (Fig. 1), which could be monitored and terminated within a few percent of a required value. A rod, B, extending from the base of the pot provided one connecting point. The upper connection was provided by rod C, initially connected to the pot by centering struts, D.

Dry, high-purity N_2 was bubbled through the monomer for 30 min prior to mixing in the initiator to 0.2 vol % and loading into the pot with the centering struts, D, in position. The cure was started at 55°C and monitored by torsion-

*Present address: Varian Associates Inc., P.O. Box 10800, Palo Alto, CA 94303, U.S.A.

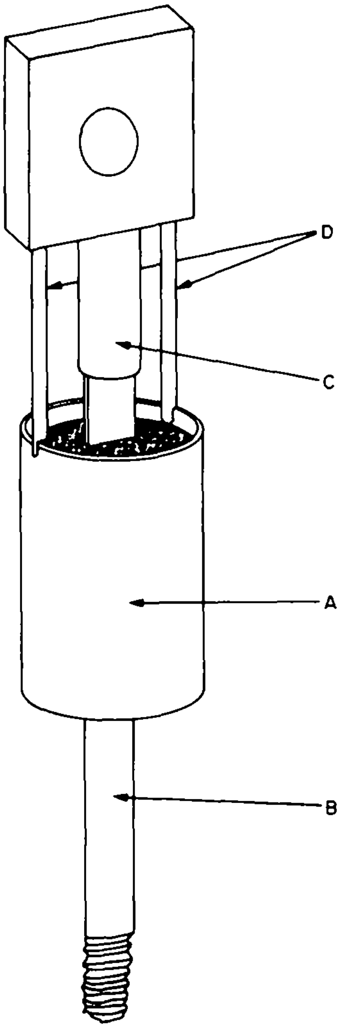

Fig. 1. Curing pot, A, with rods, B and C, to provide connections to a torsion-pendulum. Centering struts, D, are shown in position, locating the upper connecting rod. When the resin sets, the struts are removed.

pendulum measurements and terminated when the T_g corresponding to the required extent of cure was attained. Samples whose T_g exceeded 55°C were prepared by curing at the temperature of the required T_g for 4 days. The ultimate cure was attained after curing at 150°C for 3 hr after 4 days cure at 80°C.

Torsion-pendulum measurements

Once a sample had gelled, the pot could be removed from the oven and connected to the torsion-pendulum with the centering supports, D, removed. The upper connection was now made by the flattened lower part of rod, C, set axially in the cylindrical polymer sample.

The sample was usually scanned from −140°C to 50°C above the glass-transition temperature, T_g, i.e. well into the rubbery plateau region. Fast scanning was necessary at higher temperatures to minimize further curing. The period, P, and the logarithmic decrement, Δ, were measured several times at each temperature and the mean taken. This technique permitted direct monitoring of a sample being prepared and was much more sensitive than torsion-braid analysis particularly in respect to minor transitions.

Superambient temperatures were maintained with a thermostatically controlled fan-heater. Subambient temperatures were attained by allowing the apparatus to warm slowly, screened by an empty Dewar vessel, after being cooled by liquid N_2. At subambient temperatures, the system was flushed continuously by dry, high-purity N_2 to prevent condensation of moisture.

The frequency range of the torsion pendulum was 1–10 Hz.

Differential scanning calorimetry (DSC)

A Perkin-Elmer DSC 2 was used. The enthalpy of polymerization was determined on batches of monomer, previously outgassed with dry N_2, loaded in a nitrogen dry box into sealed pans with 0.2% initiator. The samples were scanned at 20°C min^{-1} until no exotherm could be detected (~520 K). Indium and lead standards were used for calibration.

The extent of cure of under-cured samples was determined from the magnitude of the exotherm (ΔH) when they were scanned to ultimate cure at 20°C min^{-1}. The extent of cure was taken at $100(\Delta H_p - \Delta H)/\Delta H_p$. Exotherms were estimated by cutting out the recorder traces and weighing the peaks. ΔH_p was determined by DSC.

PE/MAS ^{13}C-NMR measurements

The techniques, which followed Schaefer [2, 3] in all essentials, have been described previously [5]. In the present work we used a ^{1}H decoupling field of 61 kHz (1.36 G), a ^{13}C spin lock field of 60 kHz (53 G), and a recycle time of 5 sec. The temperature of the sample in the MAS probe of the Bruker CXP300 spectrometer was 298 ± 3 K. Calibration was made by $T_{1\rho}$(H) values, determined separately by conventional NMR techniques in a variable temperature probe.

In cross-polarization, spin-lock experiment the dependence of the intensity of the resonance of each C group (I) was determined as a function of the time ^{13}C atoms were held in contact with the polarized ^{1}H atoms. This is the cross-polarization time, t_{cp}. The data were fitted using the DATAFIT non-linear regression program [7] to the equation:

$$I = [S_\infty - (S_\infty - S_0)\exp\{-t_{cp}/T_{SL}\}] \times \exp\{-t_{cp}/T_{1\rho}(\mathrm{H})\} + S_0 \quad (1)$$

where T_{SL} is the time constant for the spin-locked cross-polarization process, $T_{1\rho}$(H) is the relaxation time of ^{13}C polarization in the proton rotating field, S_0 is the intensity in the absence of the cross-polarization pulse, S_∞ is the intensity which would be attained in the absence of the $T_{1\rho}$(H) relaxation mechanism.

Occasionally the four-parameter fit of equation 1 was unsatisfactory and a better fit was obtained with five parameters—the fifth replacing the S_0 at its second appearance. In rare cases where the data would not support the four or five parameter fits, somewhat inaccurate values of T_{SL} were extracted from the early points using a three-parameter fit to the term in square brackets in equation 1.

$T_{1\rho}$(H) is cited as the mean for all C groups in a sample (except the unreliable CO), since the relaxation mechanism involves the proton pool as a whole.

$T_{1\rho}$(C) was measured from the decay of the ^{13}C intensities after cross-polarization contact was broken switching off the ^{1}H rotating field. The data fit could be accommodated in the spectrometer computer.

Compression moduli were measured using a compression jig on an Instron tensile tester. Monomer was polymerized in moulds to yield disc-shaped test-samples 1 cm in diameter and 4 mm thick.

RESULTS AND DISCUSSION

^{13}C-NMR chemical shift assignments

The early onset of gelation invalidates usual techniques for obtaining high resolution ^{13}C-NMR

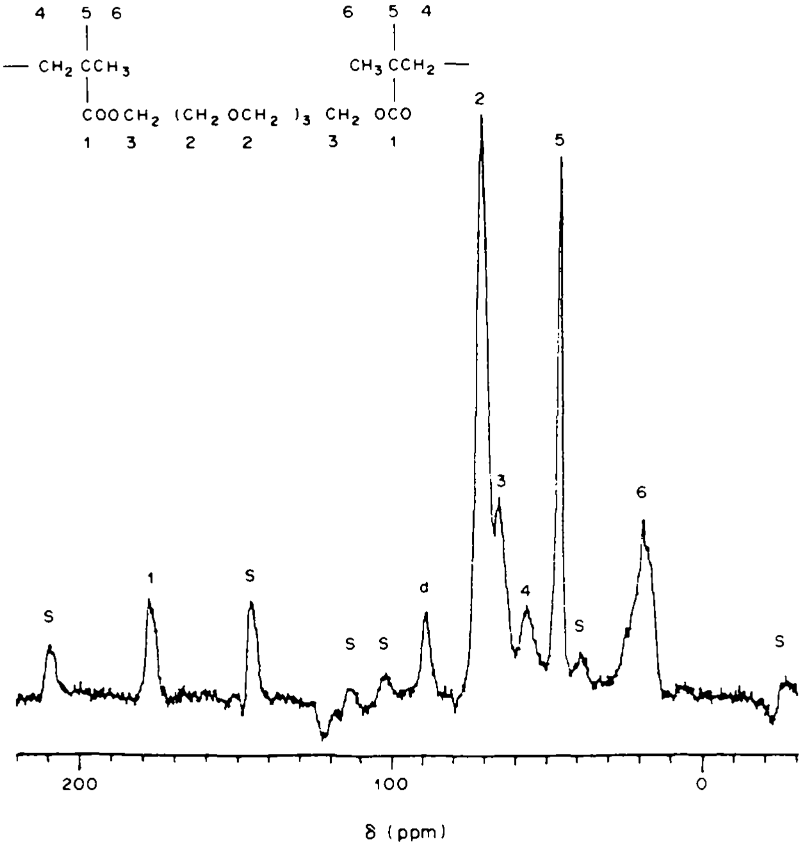

Fig. 2. PE/MAS ^{13}C-NMR spectrum of PTEGDMA at limiting cure with assignments. Spinning side-bands are labelled s, and d is the resonance of the Delrin rotor.

spectra of the polymers. Chemical shifts are only accessible by the PE/MAS experiment. Figure 2 shows the assignment of the high-resolution ^{13}C-PE/MAS spectrum of a sample of ultimate-cure PTEGDMA. Two OCH_2 resonances are resolved. The least intense, peak 3, is attributed to the end of the oxyethylene chain, the OCH_2 attached to the methacrylate chain. Peak 2 includes all OCH_2s in the interior of the oxyethylene chain. These assignments and some for other poly(diacrylates) have been reported previously [5] but it should be noted that the tabulated data in that source have the data lines for peaks 4 and 5 mutally transposed. Figure shows spinning side-bands (s). Where necessary these were suppressed using the Toss sequence [8].

Enthalpy of polymerization (ΔH_p)

This was determined by DSC. The curing exotherm was broad, with the major peak at 395 K and an incompletely resolved satellite at 415 K. The 415 K exotherm accounted for ~ 19% of the polymerization. We also observed double-peaked curing exotherms with di-, tri, and nona(ethylene glycol)dimethacrylates but not with the higher homologues. They may arise when the glass transition climbs above the curing temperature. T_g for fully cured PTEGDMA is 338 K (Fig. 3). However this was determined in a torsion-pendulum experiment

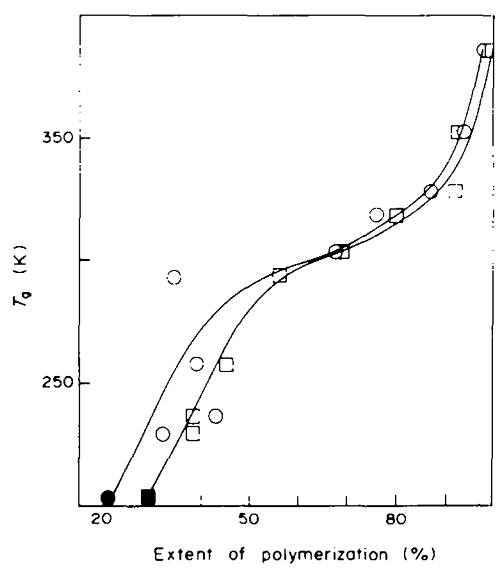

Fig. 3. Dependence of the glass-transition temperature, T_g, determined by torsion pendulum measurements (at ~ 1 Hz), on extent of cure estimated by DSC (□) or from total unsaturation determined by MAS ^{13}C-NMR techniques (○). T_g of the soft first sample was determined by DSC (■, ●).

Table 1. The dependence of dynamic mechanical and NMR parameters on extent of cure

% Cure (DSC)		28	38	38	45	56	69	80	92	93	100
% Cure (PE/MAS NMR)		21	32	43	39	34	68	76	87	94	98
% Constrained unsaturation		-	8	—		10	8	5	—	–	2
% Unconstrained unsaturation		—	61	—	--	52	23	26	—	—	0
T_g/K*		203	229	236	258	293	303	318	328	353	388
Half width of T_g/°C		--	31	37	74	>75	>110	—	—	—	153
Δ_{max}		—	1.6	0.81	0.74	0.35	0.52	—	—	-	0.34
Compression modulus/MPa		0.56	0.91	0.98	1.21	1.60	1.71	1.75	12	40.7	52.1
CO	T_{SL}/msec†	—	--	—	—	---	0.16 ± 0.02	0.17 ± 0.02	0.39 ± 0.03	0.40 ± 0.04	0.33 ± 0.02
(178 ppm)	$T_{1\rho}$(C)/msec†	—	-	—	3.77 ± 0.03	—	60.02 ± 0.02	78.14 ± 0.02	302.6 ± 0.01	323.9 ± 0.01	108.04 ± 0.01
Inner CH_2O	T_{SL}/msec†	0.12 ± 0.02	0.121 ± 0.006	0.06 ± 0.05	0.103 ± 0.006	0.085 ± 0.005	0.044 ± 0.002	0.033 + 0.001	0.042 ± 0.003	0.037 ± 0.001	0.049 ± 0.001
(70 ppm)	$T_{1\rho}$(C)/msec†	5.35 ± 0.01	5.04 ± 0.01	4.06 ± 0.01	4.42 ± 0.01	4.61 ± 0.004	3.52 ± 0.005	3.70 ± 0.005	6.08 ± 0.004	7.61 ± 0.004	8.21 ± 0.005
End CH_2O	T_{SL}/msec†	0.16 ± 0.02	0.052 ± 0.007	--	0.034 ± 0.001	0.417 ± 0.005	0.042 ± 0.006	0.0156 ± 0.0008	0.030 ± 0.001	0.025 ± 0.001	0.041 + 0.001
(65 ppm)	$T_{1\rho}$(C)/msec†	5.36 ± 0.03	1.35 ± 0.02	1.95 ± 0.02	2.60 + 0.01	1.72 ± 0.01	2.67 + 0.02	4.06 ± 0.01	5.8 + 0.005	6.95 ± 0.005	6.69 ± 0.01
CH_2	T_{SL}/msec†	—	0.087 ± 0.009	0.093 ± 0.013	0.07 ± 0.02	0.043 ± 0.005	0.015 ± 0.001	0.022 ± 0.002	0.017 ± 0.001	0.0093 ± 0.0007	0.059 ± 0.003
(56 ppm)	$T_{1\rho}$(C)/msec†	—	7.87 ± 0.02	1.09 ± 0.03	3.89 ± 0.04	2.17 ± 0.02	4.88 ± 0.02	4.08 ± 0.02	14.75 ± 0.01	12.77 ± 0.01	13.66 ± 0.01
–C–	T_{SL}/msec†	0.34 ± 0.05	0.18 ± 0.01	0.118 ± 0.009	0.20 ± 0.01	0.24 ± 0.03	0.149 ± 0.006	0.20 ± 0.02	0.19 ± 0.006	0.196 + 0.005	0.21 ± 0.01
(45 ppm)	$T_{1\rho}$(C)/msec†	10.32 ± 0.008	15.26 + 0.02	8.81 ± 0.01	19.31 + 0.06	23.48 ± 0.006	36.22 ± 0.01	51.40 ± 0.01	110.32 ± 0.02	86.04 + 0.003	130.70 ± 0.003
h-CH_3	T_{SL}/msec†	0.17 ± 0.03	0.102 ± 0.004	0.11 ± 0.01	0.033 ± 0.004	0.13 ± 0.02	0.088 + 0.003	0.107 ± 0.013	0.141 + 0.004	0.125 ± 0.021	0.14 + 0.01
(18 ppm)	$T_{1\rho}$(C)/msec†	15.35 ± 0.04	15.58 ± 0.03	16.32 ± 0.03	15.08 ± 0.03	16.93 ± 0.01	14.50 ± 0.01	17.22 ± 0.01	25.80 ± 0.005	19.32 ± 0.004	21.30 ± 0.01
Proton pool	$T_{1\rho}$(H)/msec‡	1.54 ± 0.4	1.1 ± 0.5	1.5 ± 0.7	1.7 ± 0.7	1.5 ± 0.7	2.2 ± 1.2	1.1 ± 0.4	1.8 ± 0.5	2.7 ± 0.7	2.0 ± 0.9

*By torsion pendulum at *ca* 1 Hz, except for the first which is by DSC.
†Errors cited are SE estimated from r.m.s. deviation of fit.
‡Mean of all C atoms, except CO ± SE of mean.

and is not an accurate reproduction of that prevailing under the conditions of a DSC scan. Ethylene glycol dimethacrylate showed a single curing exotherm. This resin cracks and crumbles during cure.

The enthalpy of polymerization of liquid TEGDMA was found to be $-294 \pm$ (SE) $18\ J\ g^{-1}$. As a thermodynamic reaction parameter, this value must be treated with reserve, as measurements described below suggested that apparently fully cured samples contained $\sim 2\%$ unsaturation. The value ($-97\ kJ\ mol^{-1}$) can be compared with $-104\ kJ\ mol^{-1}$ for poly(ethylene glycol)dimethacrylate [9] and $-57.5\ kJ\ mol^{-1}$ for the monofunctional 2-ethoxyethyl methacrylate [10].

Extent of cure

Extents of cure were determined by DSC, as described in the Experimental section, and by NMR.

Strictly speaking, DSC measures extents of *attainable cure* since the determination is made relative to a value of the enthalpy of polymerization, $-294\ J\ g^{-1}$ in this case, calculated on the assumption that complete conversion of monomer was attained when no further exothermic reaction could be induced by heating up to 520 K.

This appeared to be the case with the higher homologues where the NMR spectra showed no trace of residual unsaturation at ultimate cure. These were the homologues which yielded networks with subambient T_g values at full cure. The four lowest homologues, which are glassy at ultimate cure, all contained residual unsaturation even when cured until no exotherms were evident below the onset of the decomposition endotherm (~ 520 K). PTEGDMA contained 2% unsaturation at this ultimate cure. The three lower homologues, in descending order, contained 12, 18 and 15% unsaturation at ultimate cure.

Table 1 shows both the DSC and the MAS ^{13}C-NMR values of extent of cure. It should be noted that significant differences occur in some previtrification samples.

NMR could distinguish two types of unsaturation -constrained and unconstrained. The distinction between them depends on the fact that the observation of a ^{13}C resonance in the PE/MAS experiment depends on cross-polarization from nearby protons. This in turn depends on a static, dipolar interaction. It was therefore possible to distinguish between acryl groups whose motions are sufficiently constrained for them to be cross-polarized and those where isotropic molecular tumbling precluded cross-polarization. It is likely that one type, the former, included pendant glycol methacrylate chains attached to the network at one end and the other *free* glycol dimethacrylate molecules. On this basis at maximum attainable cure, PTEGDMA contained 2% unsaturation, all pendant chains. In the lower homologues, monomer appeared to remain at limiting cure the unsaturation being disposed as follows: poly[tri(ethylene glycol dimethacrylate)]: 5% in pendant chains, 7% in monomer, poly[di(ethylene glycol dimethacrylate)]: 5% in pendant chains, 13% in monomer and poly(ethylene glycol dimethacrylate): 5% in pendant chains, 10% in monomer.

This demonstration that the glassy poly(glycol dimethacrylates) contained varied amounts of monomer at limiting cure persuaded us that a characterization of the effects of cure on the dynamic molecular properties must be included in our study of structure–property relationships in the homologous series. Table 1 shows the amounts of constrained and unconstrained unsaturation, expressed as percentages of the amount of monomer originally present, for samples where the spectrum was suitable for this determination. A third estimate of percent cure can be obtained by subtracting the sum of the percentages of constrained and unconstrained unsaturation from 100.

The qualification "free" monomer used in the assignment of unconstrained unsaturation has been made in the light of recent experiments on poly(ethylene glycol dimethacrylate) [11] which show that some monomer contributes to the constrained-unsaturation content. It is presumably coordinated to, or trapped in the network. We cannot determine whether this also occurs with PTEGDMA.

Torsion pendulum measurements

Figure 3 shows the change of T_g with conversion. The first sample was too soft for torsion measurements and T_g was determined by DSC. Estimates of extent of cure by both DSC and MAS NMR are shown.

The transition became broader as conversion increased. The half width is shown in Table 1 together with the logarithmic decrement at T_g, Λ_{max}, which decreased with conversion. The broadening of the glass transition reflects a broadening of the range of segmental environments and the concomitant broadening of the distribution of cooperative, segmental mobility modes as monomer and its plasticizing effect is lost. The broadening of the range of segmental environments was also demonstrated by the lineshapes of small tracer molecule peaks in a conventional NMR experiment [12]. Other transitions are observed. One in the range 203–208 K decreased in intensity with cure, vanishing in the three high cure samples. It was assumed to be a monomer transition, probably the one at 163 K in the DSC of pure monomer. One at ~ 143 K was probably the polymer γ-transition (see below). A β-transition appeared at ~ 293 K in glassy samples, a region obscured by the breadth of the T_g in rubbery samples. There was also a water-induced transition (common in methacrylates) at ~ 170 K in glassy samples and slightly higher in the rubbery ones.

T_{SL} and $T_{1\rho}(H)$

The cross-polarisation of ^{13}C nuclei by adjacent polarized protons is assumed to be controlled by a single time-constant T_{SL}. In the spin-lock (SL) experiment [2, 3] the protons are polarized by a large static field, H_0, and then subjected to a $\pi/2$ pulse, followed by a 90° phase-shift and continuous irradiation by an r.f. field at the Larmor frequency of the protons, rotating about the H_0 direction (Fig. 4). The cross-polarization mechanism is initiated by applying a rotating r.f. field to the ^{13}C nuclei with amplitude carefully adjusted so that the energy gap for spin-flips corresponds exactly to that of ^1H (the Hartmann and Hahn condition). Cross-polarization ensues until the

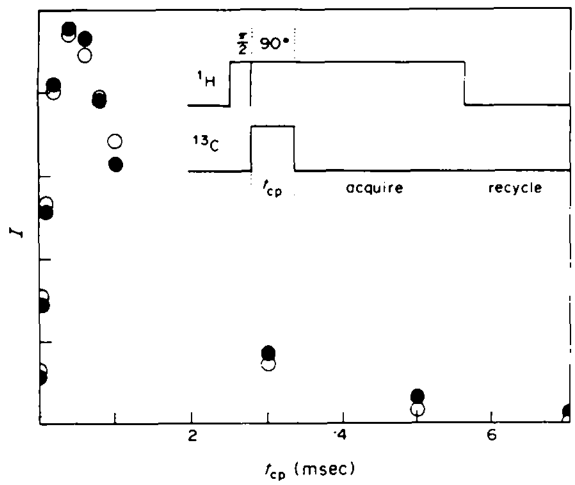

Fig. 4. The dependence of the intensity, I (arbitrary units), of the PE/MAS ^{13}C resonance 5 (quaternary) of a 45% cured resin on the spin-lock contact-time, t_{cp}: (●) observed and (○) estimated using a 4-parameter fit to equation 1. The pulse programme is also shown.

contact is broken by switching off the ^{13}C rotating field.

During the contact, the proton magnetization is decaying in its rotating field at its characteristic relaxation time $T_{1\rho}(H)$, consequently if the intensity (I) of a ^{13}C resonance is measured after increasing contact times, it will increase at short contact times as cross-polarization builds up the ^{13}C magnetization but this is overtaken at longer contact times by the decline in the proton magnetization which feeds the cross-polarisation. This can be seen in Fig. 4 where the I–t_{cp} relationship for the quarternary carbon of a 45% cured sample is shown together with the four-parameter fit according to equation 1 used to obtain estimates of T_{SL} and $T_{1\rho}(H)$.

Cross-polarization occurs through a static-dipolar coupling of proton and ^{13}C spins [2, 3] which is averaged out by isotropic molecular motion. This will be manifest in long values of T_{SL}. Low frequency motions have the greatest effect. It is believed that T_{SL} measurements provide a window on near-static components in the motion of a particular group [2].

Table 1 shows the results for the groups whose resonances were adequately resolved in a series of PTEGDMA resins of different extent of cure. The uncertainty ranges cited are the standard errors arising from the curve-fitting of the time-dependence of the ^{13}C resonance intensities in the spin-lock experiment. However when correlations are sought with extent of cure, the deviation of the measurements on some groups (Table 1) and some samples was much larger. Of the resonances, the sharp isolated quaternary carbon, 5, was consistently the most reliable; the carbonyl, 1, and acrylic CH_2, 4, most prone to large deviation. Three samples investigated are excluded from the data presented on the grounds that the dynamic parameters of all groups were devious. In a recent study of the gel structure of undercured PTEGDMA networks using the line shape of ^{13}C peaks of monomer and small tracer molecules [12], we found a similar proportion of abnormal samples. The lineshapes clearly indicated that the small molecules in the abnormal samples were distributed in two domains, one in which their isotropic motion was relatively unconstrained and one in which it was constrained. In the normal samples any inhomogeneity in the distribution of small molecules was at a level too small to detect. In two of the three samples giving devious PE/MAS dynamic parameters, the presence of separate liquid and gel phases was visibly obvious justifying their exclusion from the considered data on the grounds that they were macroscopically inhomogeneous.

Samples were spun in Delrin rotors. The T_{SL} and $T_{1\rho}$ values determined for Delrin provide a monitor for deviations in sample parameters arising from instrument and data-processing artefacts in both this and the $T_{1\rho}(C)$ series of experiments.

Figure 5 shows the dependence of T_{SL} on extent of cure. Unfortunately no one experimental parameter is wholly satisfactory as a measure of the constraining of individual group motion as the cure proceeds. T_g of the resin is an indication of molecular motion but it is cooperative motion. The DSC estimation of extent of cure is ambiguous in measuring residual unsaturation (bound and unbound) and this only as a percentage of limiting attainable cure. The constraint on group motion comes about from the increasing tightness of the network as bound unsaturation, pendant double bonds, is consumed and from the disappearance of free monomer which (see above: Torsion pendulum measurements) has a plasticizing effect. The latter is likely to be the predominant effect, except perhaps as the gel point is approached and at high cure. In Fig. 5 we correlate T_{SL} with an extent of cure based on MAS ^{13}C-NMR analysis of residual unsaturation. The correlation is

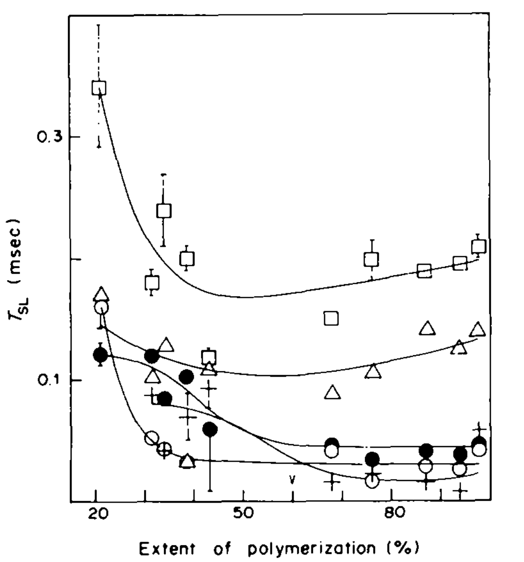

Fig. 5. Dependence of cross-polarization time-constant, T_{SL} msec, of ^{13}C resonances on extent of cure by MAS NMR. Peak 2 (inner CH_2O) is (●); 3 (end CH_2O) (○); 4 (CH_2) (+); 5 (quaternary) (□); and 6 (h-CH_3) (△). Where the standard error of T_{SL} exceeds the bounds of the symbol, it is shown. The conversion where T_g rises to probe temperature (298 K), the vitrification point, is shown by V.

smoother than that with extent-by-DSC, in contrast with the correlation of T_g by extent (Fig. 3).

The intensity of the cross-polarization interaction is short range, proportional to r_{C-H}^{-6}, and the effect is dominated by the number of nearest neighbour protons with the diminishing effects of protons within two or three bonds agreeing with their r_{C-H} values [13]. Rapid molecular motion attenuates the cross-polarization interaction. This is particularly the case with methyl groups undergoing rotation or rotatory rearrangement. Taking both effects into account, it was predicted, and observed, that cross-polarization rates have relative magnitudes: CH_3(static) > CH_2 > CH ≈ CH_3(rotating) > C(quaternary), except that no compound could be found with a static CH_3 [13]. This is what we observed (Fig. 5). The time constant for cross-polarization (T_{SL}) declines in the order: C(quaternary) > CH_3 > CH_2 for all vitrified samples. There is no significant difference between CH_2O and CH_2, which shows the relative unimportance of protons more remote than nearest neighbour; CH_2O has two next-to-nearest neighbour protons, CH_2 none.

The CH_3 resonances can be resolved into the steric triads [5]. We selected the sharpest peak for T_{SL} and $T_{1\rho}$(C) measurements. It is the middle peak of the triplet and corresponds to the heterotactic triad (hCH_3). The long T_{SL} indicates inefficient cross-polarization of $^{13}CH_3$ consistent with rotation or rotary isomerization. In the case of poly(methyl methacrylate) it is well-established [14] by a variety of dynamic measurements that the backbone methyl group is dynamically active at and below ambient temperature. This motion, usually assumed to be rotation, is believed to be responsible for the low temperature transition usually labelled γ. We have observed this transition in all poly(glycol dimethacrylates) we have tested by torsion-pendulum or torsion-braid analysis, provided the samples were scrupulously dry. The transition was usually ~143 K, a little higher than in PMMA. It was observed in both partly and fully cured PTEGDMA and in the fully cured homologues whether glassy or rubbery.

T_{SL} remained effectively constant once vitrification occurred (Fig. 5). Vitrification is often defined (e.g. Ref. 15) as the point where T_g of the curing resin climbs above ambient temperature. The MAS probe temperature was 298 K so, if vitrification is defined in terms of T_g (1 Hz) (Fig. 3), this occurred at ~60% conversion (by either method).

T_{SL} of the quaternary C was effectively constant except for the lowest cure sample (26%). Trends dependent on a single sample must be treated with caution. If this one was real, it was probably a consequence of large amplitude motions still being present at this low cure. The cross-polarization mechanism available to a quaternary C is dependent on next-to-nearest-neighbour-protons and this weak interaction may therefore be sensitive to large amplitude motion. The decline of T_{SL} for CH_2 and the two CH_2O peaks is more gradual. It would seem that the mobility of the end CH_2O becomes constrained earlier than the inner CH_2O groups.

$T_{1\rho}$(H) values for each group are shown in Table 1. The relaxation of the proton magnetization in its rotating field is a process dominated by spin-diffusion through the proton pool. $T_{1\rho}$(H) therefore gives no information about group motions. It is governed by the motions of the proton pool of the whole sample if it is homogeneous, or of the individual phases if it is heterogeneous. Our results were consistent with a single proton pool dominating each sample and the motions responsible for the $T_{1\rho}$(H) relaxation did not change significantly as the cure progressed.

$T_{1\rho}(C)$

In this experiment the spin-lock contact was established but terminated by switching off the proton rotating field and allowing the ^{13}C polarization to decay in its own rotating field for a determined interval. This was terminated by switching off the carbon field, restoring the proton field and acquiring the data. The decay in the ^{13}C magnetization in its rotating field was assumed to be controlled by a single relaxation-time, $T_{1\rho}$(C), which was determined by a 3-parameter fit of the dependence of line-intensity on the decay time. Since only one time constant is involved the statistical reliability of the values of $T_{1\rho}$(C) determined is greater than that of T_{SL}. However as in the case of T_{SL}, anomalous peaks and anomalous samples were occasionally encountered which deviated from any reasonably smooth correlation by many standard deviations (Table 1). The great question concerning the $T_{1\rho}$(C) relaxation [2, 16–20] is the extent to which it is brought about by heteronuclear spin spin coupling, which gives no information about molecular dynamics, and spin–lattice processes in the rotating frame which provide an observational window onto group motions with components in the middle decade of the kHz range, according to the selected rotating field (60 kHz in our experiments). The second question is the extent to which the spin–lattice component of the whole molecule is dominated by the methyl rotation relaxing other carbons through long range C-H dipolar interaction. This has been reported to occur with semicrystalline polypropene [19] and amorphous PMMA [21, 19]. Our experiments have bearing on both these questions.

The most striking feature of the change in $T_{1\rho}$(C) during cure (Fig. 6) was the restriction of the relaxation mechanism after vitrification. It was strongest at the acrylate backbone groups. During this process, $T_{1\rho}$(C) lengthened 7-fold at the quaternary carbon, 4-fold at CH_2, 3-fold at the end CH_2O and doubled at inner CH_2O. A much less significant restriction on relaxations was observed at CH_3. Whatever the relative importance of spin-spin and spin-lattice relaxations in determining the magnitude of $T_{1\rho}$(C) may be, the contribution of the latter is significant because the effect observed can only arise from a damping of molecular motion in the relevant frequency range.

The effect was strongest at the quaternary C and declined with increasing separation of the group from quaternary C, except in the case of CH_3 where it was small. Post-vitrification cure clearly does not have much effect on CH_3 motions in the mid kHz range at ambient temperature. The more drastic effects observed with the $T_{1\rho}$(C) relaxation of other groups were therefore not manifestations of changes in CH_3 motion.

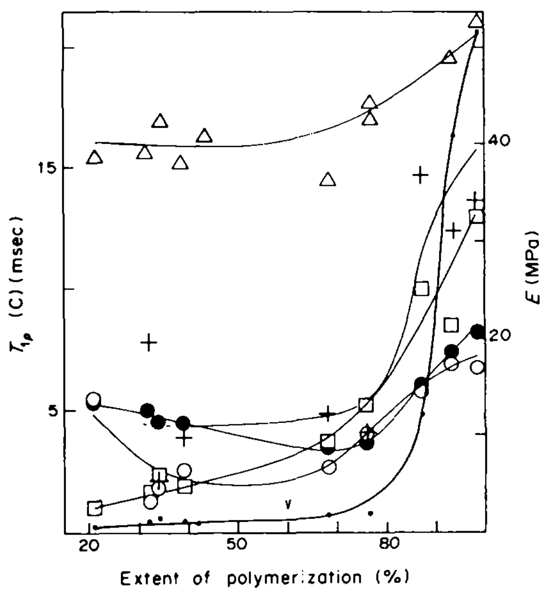

Fig. 6. Dependence of the relaxation time of ^{13}C resonances in a 60 kHZ rotating field, $T_{1\rho}$(C) msec, on extent of cure by MAS NMR. Peak 2 (inner CH_2O) is (●); 3 (end CH_2O) (○); 4 (CH_2) (+); and 6 (h-CH_3) (△). For peak 5 (quaternary) (□) represents $T_{1\rho}$(C) msec/10. Standard errors on $T_{1\rho}$(C) do not exceed the bounds of the symbols. The dots represent the compression modulus, E (MPa). V indicates the vitrification point.

Compression-modulus correlations

The pot torsional-pendulum experiment was not suitable for making measurements on samples of standard geometry at different extents of cure, so we examined the change of compression-modulus with extent of cure. The initial slope of the stress–strain plot, taken at 0.3% strain, was measured for samples compressed at 2 mm min $^{-1}$.

The modulus increased slowly and steadily until the cure exceeded 80% when it increased 30-fold to its ultimate value (Fig. 6). A sudden change in compression modulus during cure has been observed also for tri(ethylene glycol)dimethacrylate [22]. This lower homologue yields a network with a shorter flexible link and the modulus starts to rise earlier in the cure than it does with TEGDMA.

The most interesting feature of these results is that the step in the compression–modulus–cure curve (Fig. 6) coincides with similar ones in the $T_{1\rho}$(C)–cure curves and the final decline of T_{SL} for inner CH_2O and CH_2 groups to its limiting value (Fig. 5). Correlations between compression modulus and T_{SL} and $T_{1\rho}$(C), of all groups except CH_3, can be perceived, despite the scatter on the time constants and the relative insensitivity of E over 80% of the cure range.

CONCLUSIONS

The results have no direct bearing on the question of the relative contribution of the spin-spin relaxation mechanism to the magnitude of $T_{1\rho}$(C) of different groups, though it is conceivable that this may be the reason why it is 10 times longer at quaternary C than at CH_2. What the results do show is that the motion-dependent spin–lattice mechanism is sufficiently important to give a clear indication of *changes* in group motions such as the sudden constraint that affects all groups, except possibly CH_3, in the immediate post-vitrification period.

While the 60 kHz components, which control the spin–lattice contribution to $T_{1\rho}$(C), become suddenly constrained at, or just after vitrification, the lower frequency components governing T_{SL} become constrained earlier. In all cases the limiting high-conversion value is reached before vitrification, though in the case of the inner CH_2O the final decline takes place later than other groups. The constraint on the 60 kHz components continues to increase, though at a lower rate than that in the immediate post-vitrification period, right up to ultimate cure. T_g also increases right up to ultimate cure demonstrating the contribution of mid kHz motions of individual groups to the cooperative motions which determine the glass transition.

The most striking result is the association of vitrification, defined by a macroscopic property such as bulk modulus determined by a near static technique, with a sudden constraint on the mid-kHz components of group motion, while low frequency group motions are no longer relevant. This again suggests that it is the mid-kHz group motions which are responsible for lower frequency cooperative motion.

Vitrification can be attributed to two molecular processes—the tightening of the network as polymerization continues within the already gelled resin and the concomitant loss of the plasticizer action of monomer. In connection with this latter aspect of vitrification, it is interesting to note the $T_{1\rho}$(C) measurements have demonstrated that added plasticizers act by releasing mid-kHz components of group mobility of polycarbonates [23].

The CH_3 group is least affected by the progress of the cure. In the T_{SL} frequency domain no trend emerges from the data-scatter. In the $T_{1\rho}$(C) domain a slight, progressive, post-vitrification restriction is probably significant. Variable-temperature MAS experiments on amorphous poly(methyl methacrylate) indicate that a minimum in $T_{1\rho}$(C) for CH_3 between 140 and 200 K is reflected in minima in the values for CO, OCH_3 and quaternary C [19]. This was assumed to indicate that the motions of CH_3 were relaxing other carbons through long-range C–H dipolar interactions. The changes in relaxation rates of other carbons, observed in our ambient temperature experiments, being larger than those of CH_3 cannot originate at that group. We conclude that they arise from changes in the motion of the groups themselves, particularly as the group which shows the greatest change is unprotonated. The implication that the constraint on motion acts most strongly at quaternary C and is felt less strongly by other groups (except CH_3) the further they are removed from quaternary must be treated with caution; the caution is given by Schaefer [3] that one cannot, from the magnitude of $T_{1\rho}$(C) alone, distinguish between small amplitude motions in tune with the frequency of the observational window and large amplitude motions somewhat off-tune.

Acknowledgement—We acknowledge the support of the Australian Research Grants Scheme.

REFERENCES

1. A. M. North, *Molecular Behaviour and Development of Polymeric Materials* (Edited by A. Ledwith and A. M. North), p. 368. Chapman & Hall, London (1974).
2. J. Schaefer, E. O. Stejskal and R. Buchdahl, *Macromolecules* **10,** 384 (1977).
3. J. Schaefer and E. O. Stejskal, *Top. ^{13}C NMR Spectrosc.* **3,** 284 (1979).
4. T. Okada and K. Kaji, *Jap. Atomic Energy Res. Inst.* **5030,** 77 (1974), cited in *Nucl. Sci. Abst.* **32,** 1634 (1975) (citation no. 16839).
5. P. E. M. Allen, G. P. Simon, D. R. G. Williams and E. H. Williams, *Polym. Bull., Berlin* **11,** 593 (1984).
6. W. N. Guljawzew, Ju. M. Siwergin, S. M. Kirejewa, Ju. Selenew and A. A. Berlin, *Plaste Kautsch* **18,** 740 (1971).
7. M. E. Gál, G. R. Kelly and T. Kurucsev, *J. chem. Soc. Faraday Trans. II* **69,** 395 (1973).
8. W. J. Dixon, J. Schaefer, M. D. Sefcik, E. O. Stejskal and R. A. McKay, *J. Magnet. Reson.* **49,** 341 (1982).
9. J. E. Moore, *Chemistry and Properties of Crosslinked Polymer* (Edited by S. S. Labana), p. 535. Academic Press, New York (1977).
10. K. J. Ivin, *Polymer Handbook* (Edited by J. Brandrup) 2nd edn, p. II 424. Wiley, New York (1975).
11. P. E. M. Allen, D. Bennett, G. P. Simon, D. R. G. Williams and E. H. Williams, unpublished.
12. G. P. Simon, P. E. M. Allen, D. R. G. Williams and E. H. Williams, *Eur. Polym. J.* **21,** 877 (1985).
13. L. B. Alemany, D. M. Grant, R. J. Pugmire, T. D. Alger and K. W. Zilm, *J. Am. chem. Soc.* **105,** 2133, 2142 (1983).
14. N. G. McCrum, B. E. Read and G. Williams, *Anelastic and Dielectric Effects in Polymeric Solids*. Wiley, New York (1967).
15. J. B. Enns and J. K. Gillham, *Adv. chem. Ser.* **203,** 27 (1983).
16. D. L. VanderHart and A. N. Garroway, *J. chem. Phys.* **71,** 2772 (1979).
17. J. Schaefer, E. O. Stejskal, T. R. Steger, M. D. Sefcik and R. A. McKay, *Macromolecules* **13,** 1121 (1980).
18. G. Hempel and H. Schneider, *Polym. Bull., Berlin* **6,** 7 (1981).
19. W. W. Fleming, J. R. Lyerla and C. S. Yannoni, *Am. chem. Soc. Symp. Ser.* **247,** 83 (1984).
20. J. Schaefer, M. D. Sefcik, E. O. Stejskal and R. A. McKay, *Macromolecules* **17,** 1118 (1984).
21. H. T. Edzes and W. S. Veeman, *Polym. Bull., Berlin* **5,** 255 (1981).
22. M. P. Berezin and G. V. Korolev, *Vysokomolek. Soedin.* **A22,** 1872 (1980); *Polym. Sci. U.S.S.R.* **22,** 2053 (1980).
23. L. A. Belfiore, P. M. Henrichs, D. J. Massa, N. Zumbulyadis, W. P. Rothwell and S. L. Cooper, *Macromolecules* **16,** 1744 (1983).